R as an environment for data mining of process mineralogy data: A case study of an industrial rougher flotation bank

Kupka, N.; Tolosana Delgado, R.; Schach, E.; Bachmann, K.; Heinig, T.; Rudolph, M.;

Originally published:

January 2020

Minerals Engineering 146(2020), 106111

DOI: https://doi.org/10.1016/j.mineng.2019.106111

Perma-Link to Publication Repository of HZDR:

https://www.hzdr.de/publications/Publ-29555

R as an environment for data mining of process mineralogy data: a case study of an industrial rougher flotation bank

Nathalie Kupka[a,1], Raimon Tolosana-Delgado[a], Edgar Schach[a],

Kai Bachmann[a], Thomas Heinig[a], Martin Rudolph[a]

[a] *Helmholtz Institute Freiberg for Resource Technology, Helmholtz Zentrum Dresden-Rossendorf, Chemnitzer Straße 40, 09599 Freiberg, Germany*

[1]*Corresponding author, n.kupka@hzdr.de / sternath@gmail.com*

Abstract

Through a series of in-house routines of R, an open-source programming language for statistical computing, statistical analysis is applied to automated process mineralogy data to describe the performance of an industrial scheelite rougher flotation bank. These routines allow 1) freeing the user from the limitations of the menu-driven built-in processing and spreadsheet-based analyses routines; in particular when processing data from several streams, and 2) a more flexible manipulation of the data at any level of aggregation.

In an illustration case study, it was determined that ideally floating scheelite particles are coarser than 40 µm and are more than 40% liberated. Most of the scheelite lost to the rougher tailings stream is either ultrafine or coarse with little surface liberation and associated with silicates. More importantly, the presence of a depressant does not permit the selective flotation of scheelite from other semi-soluble salt-type minerals such as calcite. This is linked to particle size, as there appears to be some overgrinding before the rougher flotation. While the impact of the depressant requires more observation, less fine grinding could already potentially improve the concentrate grade and decrease operational costs.

Keywords: rougher flotation, R, automated mineralogy, statistical analysis

1. Introduction

Automated mineralogy is now widely used in the mining industry to provide detailed mineralogical information to improve ore characterization, process understanding, design and optimization. It is regularly demonstrated that the application of automated mineralogy leads to process improvements (Buchmann et al., 2018; Lotter, 2011; Pereira et al., 2019; Quinteros et al., 2015). Although automated mineralogy is a powerful tool, the data obtained could be explored in even more depth with modern computing capacities. However, as far as publications go, there are very little attempts at using data mining to analyze automated mineralogy data and usually only for a very specific topic (Vos et al., 2015).

The aim of this paper is to illustrate the potential use of R — a programming language for statistical computing and data mining (RCoreTeam, 2016) — in large scale evaluation of automated mineralogy data. Even though the idea of using process mineralogy within geometallurgical models for flotation circuit performance evaluation is not new, it appears to be limited by its capacity to identify the recoverability of different particle types (Pereira et al., 2019) or by the number of particles. Therefore, statistical analysis is expected to lead to a more in-depth assessment of the process by:

- Going beyond the limitations of both menu-driven automated mineralogy software and spreadsheet programs, for calculation and data plotting;
- Allowing the repeated analysis of hundreds of thousands of particles, also in parallel, for entire flowsheets or time series;
- Manipulating the data at any level of aggregation required: i.e., as conventional classes or bins, to examine bulk properties and individual particles.

Following on the work on cassiterite particle tracking by Schach et al. (2019), data gained during an analytical investigation of an industrial scheelite ($CaWO_4$) rougher flotation bank are used as an illustrative case study. Beyond stream characterization, the objective of this example is to understand the behavior of scheelite across the rougher bank, especially in relation to other semi-soluble salt-type minerals such as calcite, apatite and fluorite (Rao and Forssberg, 1992). These gangue minerals receive specific attention, as they exhibit similar surface properties and thus behave like scheelite in froth flotation, leading to increased contamination in the concentrates (Kupka and Rudolph, 2018). The R-based analysis should allow for a faster, more precise, and flexible characterization of the ideal scheelite particles during the rougher flotation of the ore investigated.

2. Material and Methods

Three rougher flotation streams of a scheelite beneficiation plant were investigated using granulometric, chemical, and mineralogical analyses (Figure 1). The rougher bank is divided into 6 streams, i.e., feed, three intermediate rougher concentrates, named Cells 1–4, 5–8, and 9–12, the combined rougher concentrate, and the rougher tails. Each block of cells contributes roughly one third of the rougher concentrate mass. The mass recovery of the rougher concentrate is about 33%. The rougher concentrate grade is 2.6% WO3 and tungsten recovery is 96.5%.

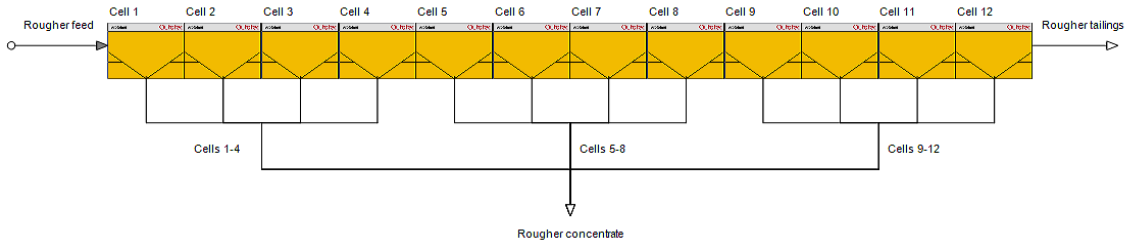

Figure 1: Streams involved in the rougher flotation bank analysis

The reagent regime mainly consists of fatty acid type collectors and the depressant quebracho, a tree tannin extract. Quebracho is expected to depress other salt-type minerals, mainly calcite, at the natural pH of the ore (about 9). The material and methods used are described below.

2.1. *Elemental assaying*

The tungsten grades were analyzed directly by the mine with XRF (X-Ray Fluorescence) while ALS Global® conducted the major oxides analysis by ICP-AES (Inductively coupled plasma atomic emission spectroscopy, method number: MS-ICP06).

2.2. *Mineral Liberation Analysis (MLA)*

Representative sample powders were prepared as A-side grain mounts (Heinig et al., 2015) and carbon coated. MLA is a FEI Quanta 650F scanning electron microscope equipped with two Bruker Quantax X-Flash 5030 EDX detectors and ThermoFisher/FEI's MLA Suite 3.1.4 for automated data acquisition (Fandrich et al., 2007). XBSE measurements for the six streams were conducted at the Helmholtz Institute Freiberg at an accelerating voltage of 25kV and a beam current of 10nA. No size-by-size samples were examined for this bank due to cost and time constraints.

MLA particle size distributions were compared with physical screen size distribution analyses to estimate the reliability of the data and to reduce the bias of virtual sizing discussed in the literature (Greet, 2013). Furthermore, even if the MLA tends to underestimate the amount of fines and ultra-fines in some streams, some authors noted that this does not prevent the user to reach similar diagnostic conclusions as with sized samples (Rolando and William, 2014).

In this study, particle sizes are defined by the maximum dimension length. Surface liberation has been calculated by dividing the total length of the target mineral at the outer perimeter of a particle by the perimeter of said particle. The colors applied to the minerals and the mineral groups were based on the “Butcher Color Scheme”, which is a widely accepted color scheme for automated mineralogy data (Butcher, 2015).

Finally, from an MLA-based classification point of view, anorthite, the calcium-rich end member of the sodium-calcium plagioclase solid solution is considered separately from the rest, denoted as albite. This was done in order to determine the impact of the calcium content in the silicates during flotation. Indeed, the flotation behaviour of calcium-containing silicates in scheelite flotation has never been looked at before even though they could potentially be receptive to scheelite collectors (Kupka and Rudolph, 2018). In the current classification, plagioclase with less than 1% Na and high contents of Al and Ca were automatically classified as anorthite. Over 1% Na, the mineral is classified as albite. The thresholds are arbitrary and were used for the purpose of this study only.

2.3. *R analysis*

Once MLA data source files are generated, they are converted to an SQL database before being imported into R. Using a series of in-house R routines, various particle descriptors and performance indicators are calculated. R was selected as a programming language because it is free, open-source and together with Python, the most popular language used by data analysts and data scientists (Kopf, 2017). R is faster and more flexible than a spreadsheet program: all calculations for one stream took

less than 2 minutes, even with several hundreds of thousands of particles; any task, once properly programmed, can be applied systematically and does not need to be rewritten. Moreover, the scripts and source codes remain as a logbook of what has been done, for documentation and traceability.

2.4. *Mass Balance*

Mass balance of the flowsheet for the mass, water and mineral flows was conducted with HSC Sim 9.1.1 (Outotec, Finland) with the Non-Negative-Least-Square Method (NNLS) and forcing a total mineral composition to 100%. Unless otherwise specified, all the data presented have been mass balanced by calculating the data with R, exporting it to HSC and reimporting it in R. It should be noted that HSC does not yet allow the mass balancing of classes other than size or composition. Thus, surface liberation classes and shape classes were mass balanced as mass fractions in separate mass balances.

2.5. *Entrainment calculations*

An entrainment factor EF for a mineral of size class *i* can be calculated for the gangue minerals based on the formula of Yianatos and Contreras (2010), which is the ratio of R_G the recovery of the free gangue particles and R_w the water recovery. For entrainment calculations, particles considered free have over 95% free surface. To take into consideration the influence of particle shape, a modified entrainment factor for a particle shape class *j* was calculated using the equation from Little et al. (2016):

$$EF_{i,j} = \frac{R_{G,i,j}}{R_w} = \frac{m_{c,j}}{m_{f,j}} * EF_i$$

Where $m_{c,j}$ is the mass of the mineral in the particle shape class in the concentrate and $m_{f,j}$ is the mass of the same mineral in the particle shape class in the feed.

2.6. *Particle shape factors*

Two shape parameters - circularity and roundness - were calculated based on the method by Pourghahramani and Forssberg (2005). For a more accurate representation of particle shape factors and a more reliable relation to entrainment, only particles with over 95% free surface were taken into account in order to decouple the effect of particle shape from surface liberation and mineral association.

Circularity is the ratio of the actual perimeter of the particle to the perimeter of the equivalent circle (Pourghahramani and Forssberg, 2005). A sphere has a circularity of 1. Circularity is almost identical to the calculation of angularity suggested by Vizcarra et al. (2011). Therefore, it can be expected that particles with high circularity values are more angular. Roundness compares the surface of the particle to the surface of the disc of maximum ferret diameter (Pourghahramani and Forssberg, 2005). The greater the roundness value, the less elongated and the more rounded the particle is.

Finally, the MLA form factor was also taken into account. It compares the outline rectangle to the calculated average polygon (FEI, 2014). The closer to zero, the closer the particle outline is to a perfect square. The MLA form factor is different than what is usually understood by form factor, e.g. a ratio of the surface of the particle to the surface of the disc with the same perimeter (Pourghahramani and Forssberg, 2005).

3. Particle descriptors derived from automated mineralogy

3.1. *General mineralogical composition*

The first information readily available through automated mineralogy is the mineralogical assemblage. The minerals of the ore are grouped as follows: phyllosilicates, quartz, scheelite, other semi-soluble salt-type minerals (abbreviated semi-solubles), other silicates, sulfides and trace minerals (Table 1). These groups are flexible and each mineral can be examined individually or within any required group.

Table 1: Mineralogical list of the ore (the main mineral constituting the group is underlined)

Groups	Minerals
Phyllosilicates	Biotite, muscovite, serpentine
Quartz	
Scheelite	
Semi-solubles	Ankerite, apatite, calcite, fluorite
Silicates	Albite, anorthite, augite, cummingtonite, hornblende, epidote, orthoclase, titanite

Sulfides	Arsenopyrite, bismuthinite, chalcopyrite, molybdenite, pentlandite, pyrite, pyrrhotite, sphalerite
Trace	Hematite, ilmenite, rutile, zircon

Figure 2 presents the mineralogical composition of the rougher bank streams. Run-of-mine grades of scheelite, calcite, sulfides and apatite are 0.6, 1.5, 1.2 and 0.3%, respectively. Due to the recirculation of cleaner tailing streams within the beneficiation plant, these minerals are enriched in the rougher feed to 1.4, 11, 6.1 and 1.1%, respectively.

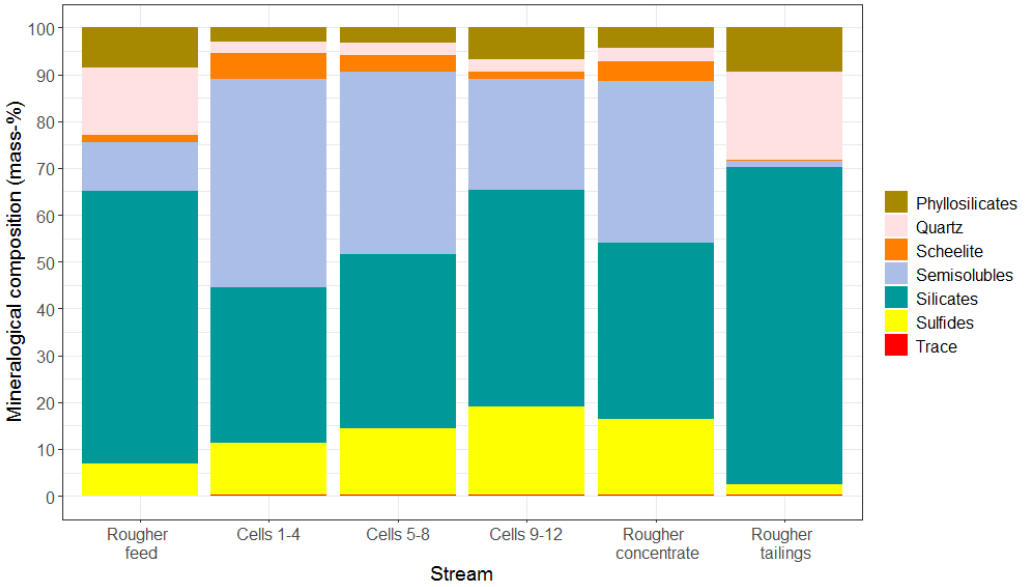

Figure 2: Mineralogical composition of the different streams (Feed, concentrates of the cells 1-4, 5-8 and 9-12, rougher concentrate and rougher tailings)

The concentrates of the three cell flotation streams are mainly composed of semi-soluble salt-type minerals, silicates and sulfides, which comprise about 90% in each stream. Scheelite is present at about 7, 4 and 2%. The main contaminants are semi-soluble salt-type minerals. Their grades in each stream are 6, 9 and 14 times higher than that of scheelite.

3.2. *Scheelite particle size*

As expected, flotation concentrates are finer than the tailings. The d_{95} of the streams is 150 µm for the concentrate of Cells 1-4, 180 µm for the other concentrates, 215 µm for the rougher feed and 250 µm for the tailings, similarly to the “fresh” feed without the recirculation of the cleaner tailings.

The mineralogical composition per particle size class of a stream, here the rougher feed, can be determined using MLA. However, using R, the mineral composition per particle size class can be calculated for quantiles, where each quantile represents 10% of the sample mass (Figure 3). Approximately 50% of the feed of the rougher bank is below 10 µm and only 10% is over 34 µm with a maximum particle diameter at 890 µm. As a brittle mineral scheelite is typically concentrated in the finer fractions, along with the phyllosilicates, while semi-soluble salt-type minerals are coarser. Silicates, quartz and sulfides are relatively evenly distributed across the particle size classes.

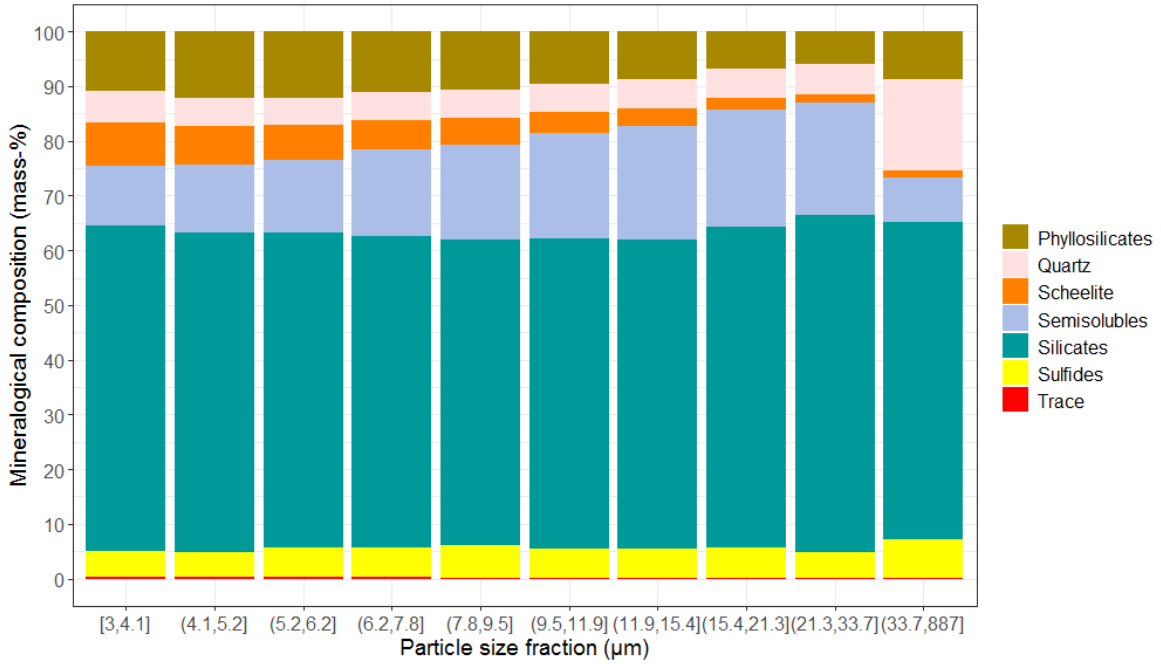

Figure 3: Mineralogical composition of the rougher feed per quantiles (each bar represents 10% of the sample mass)

The mineralogical composition per quantiles for the other streams investigated are presented in Annex 1. The graphs show that over time, the combined concentration of the groups phyllosilicates and silicates increases, with these minerals becoming the main gangue minerals. Sulfides float constantly. The rougher tailings contain very little of the semi-soluble salt-type minerals, regardless of the particle size and is the only output stream to display larger amounts of quartz.

In general, given that all particles are accessible individually within the database, it is possible to calculate any classes wanted by the user, for example the mineral assemblage weighted by a mineral or based on another property than particle size.

3.3. *Scheelite surface liberation characteristics and mineral association*

The surface liberation of a mineral and its associations have an important impact on how a mineral behaves during flotation. Figure 4a presents the kernel density estimation weighted by mass of scheelite reporting to specific surface liberation classes versus particle size in each cell block. The kernel densities of the three concentrates are plotted based on the method of Schach et al. (2019) who explain that a kernel density estimation is the estimation "*of the probability $f_{xy}(x_0, y_0)$ of having a particles with properties (x_0, y_0) in that particular stream.*" It shows clearly that most of the floated scheelite is well liberated, while over time coarser middlings particles float less and finer less liberated particles float more.

A more traditional approach would be to calculate the recovery of scheelite depending on surface liberation classes. A high liberation is not necessarily required to reach high recovery (Figure 4b) but it impacts the speed of flotation: highly liberated scheelite is mostly recovered in the first cells while less liberated scheelite is recovered in the last cells, e.g. at a longer residence time. Surface liberation is therefore divided into three classes: 0-40% locked or heavily contaminated scheelite-particles, 40-80% middlings and 80-100% liberated scheelite.

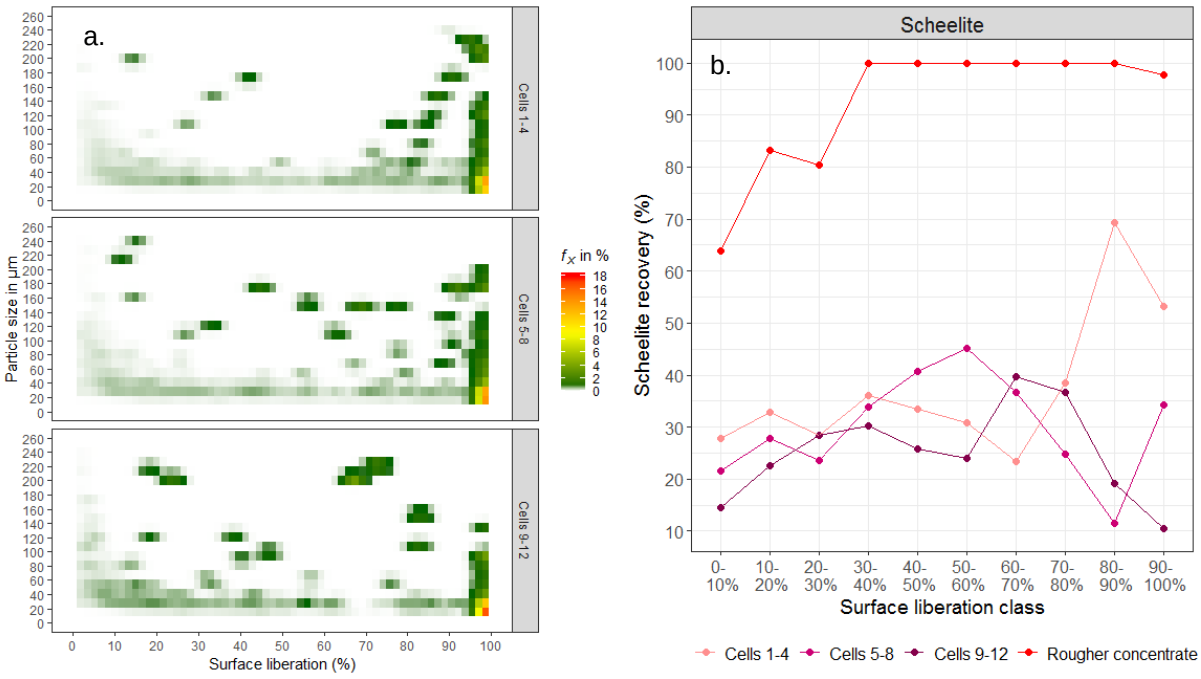

Figure 4: a) weighted kernel density estimation of scheelite surface liberation against its size and b) scheelite recovery depending on the surface liberation class and over time (lines are to guide the eye)

Figure 5 displays a more comprehensive representation of the surface liberation and mineral association of scheelite depending on its particle size. Scheelite is very well liberated in the rougher feed as well as very fine. Most of the scheelite lost to the rougher tailings stream is either ultrafine or coarse with little surface liberation and associated with silicates. An association with sulfides, semi-soluble salt-type minerals and trace minerals is not an obstacle to the flotation of scheelite as shown by the rougher concentrate.

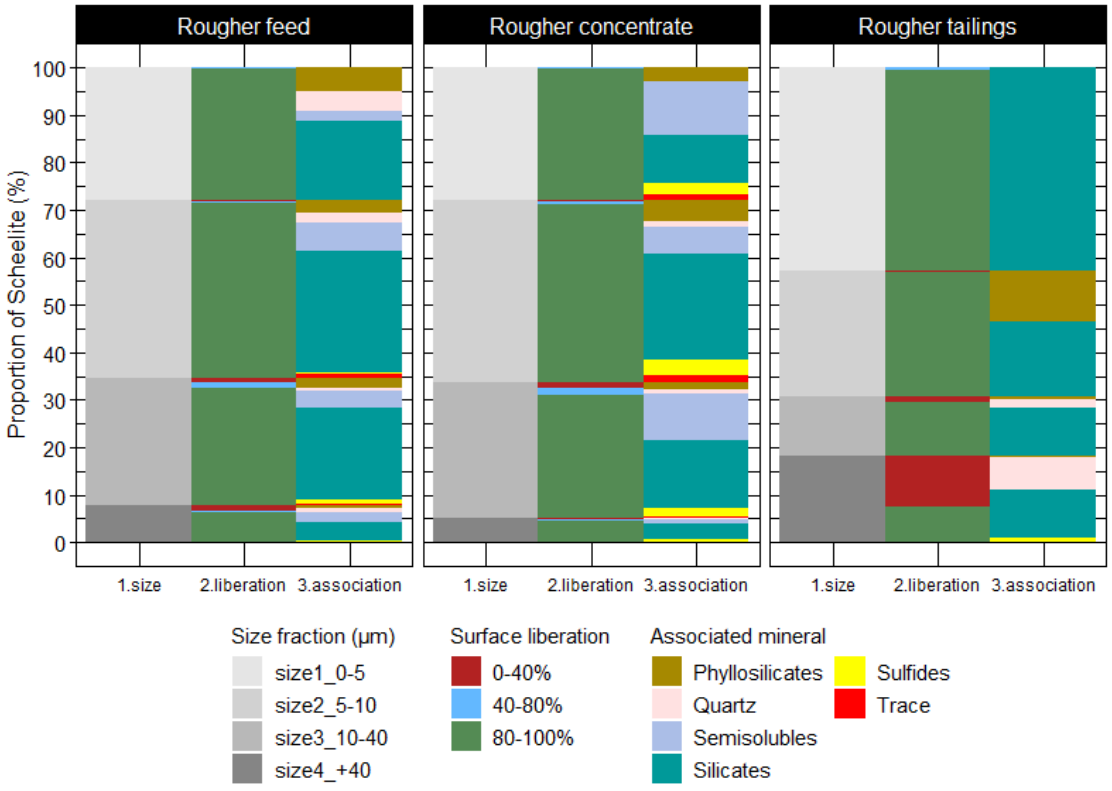

Figure 5: Proportion of the surface liberation and mineral association of scheelite depending on its size fraction for the rougher feed, the rougher concentrate and the rougher tailings

3.4. *Particle shape*

Particle shape descriptors have gained wider acceptance in the flotation community even though there is no consensus on shape effects. Vizcarra et al. (2011) noted that particle shape properties are "*significant only for minerals with slow flotation kinetics […]*" and are more relevant to gangue minerals. Few studies were conducted on particle shape related to mechanical entrainment. Wiese et al. (2015) showed that ballotini (spherical glass beads) had lower entrainment as compared to elongated wollastonite fibrous particles. The study showed a close relationship of particle shape and recovery due to entrainment increasing with increasing aspect ratio. The opposite was observed by Little et al. (2016) in a chromite entrainment study at a platinum concentrator, where rounder particles reported more to the concentrate.

Figure 6 shows the mean of each shape factor weighted by mass for the most abundant gangue minerals. It appears that most gangue minerals are less and less round over time and show higher roundness and lower form factor in the concentrates than in the tailings. Biotite and serpentine show lower roundness, a higher form factor and high circularity compared with other gangue minerals, e.g., they are more elongated, less square and more angular, which is to be expected from phyllosilicates.

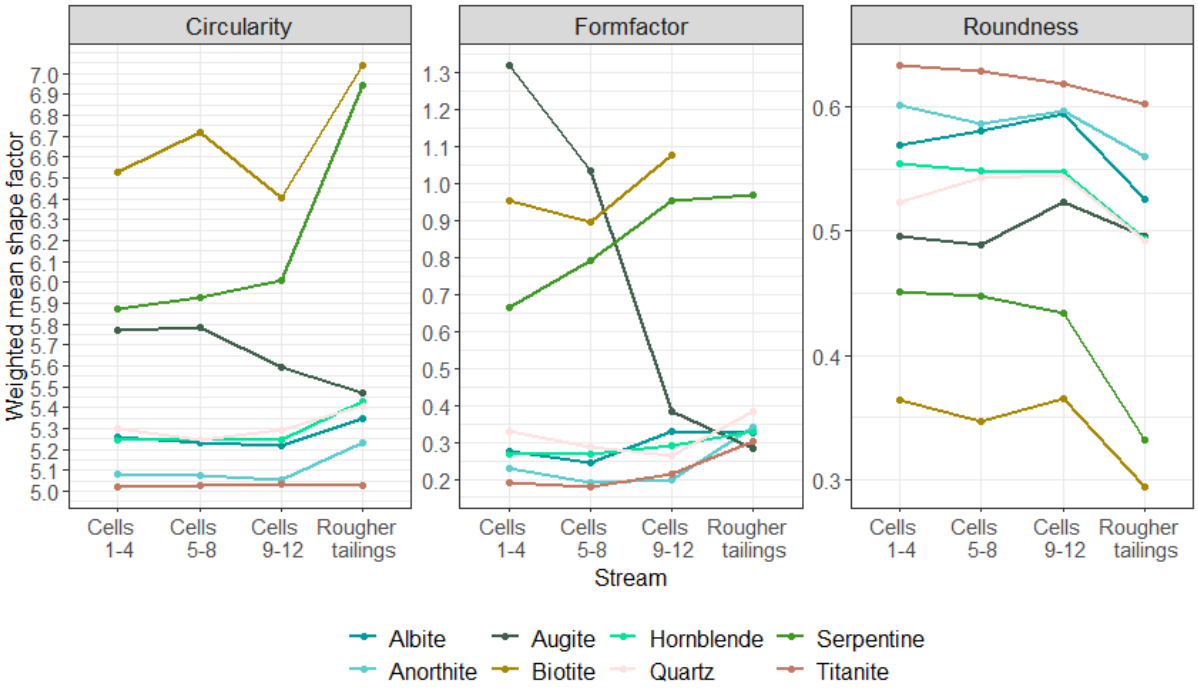

Figure 6: Weighted mean shape factor per stream and per mineral (lines are to guide the eye)

4. Flotation performance indicators

Particle descriptors derived from automated mineralogy give a good overview of how scheelite and the gangue particles behave in the rougher flotation. These descriptors can afterwards be used to calculate performance indicators, in order to identify potential weaknesses in the flowsheet.

4.1. *Kinetics*

The mineralogical composition data allow the calculation of the recoveries of the different minerals over the residence time (Figure 7a). Scheelite is recovered at 96.5%. Along with the semi-soluble salt-type minerals, it is part of the faster floating components, as they are already well enriched in the concentrates of the first eight cells. Sulfides are easily activated with fatty acids, hence their increasing rate over the flotation bank. The other minerals seem to float mechanically through entrainment, as indicated by their linear behavior.

The separation efficiency SE is an index combining concentrate recovery and grade aiming at evaluating the metallurgical efficiency of the separation, the equation of which can be found in Wills and Finch (2016), p11. The separation efficiency decreases intensely over time as true flotation of the valuable and other salt-type-type minerals is progressively taken over by entrainment of the gangue. The total separation efficiency is still measured at 65.6% for the rougher concentrate. In general, the depressant does not permit the selective separation of scheelite from other semi-soluble salt-type minerals or sulfides (Figure 7b). The low recovery of silicates as compared to scheelite is independent

of the depressant, as quebracho is not expected to depress silicates. It is not possible to say if the situation would have been worse without the addition of quebracho or if the depressant dosage is not properly calibrated to the situation.

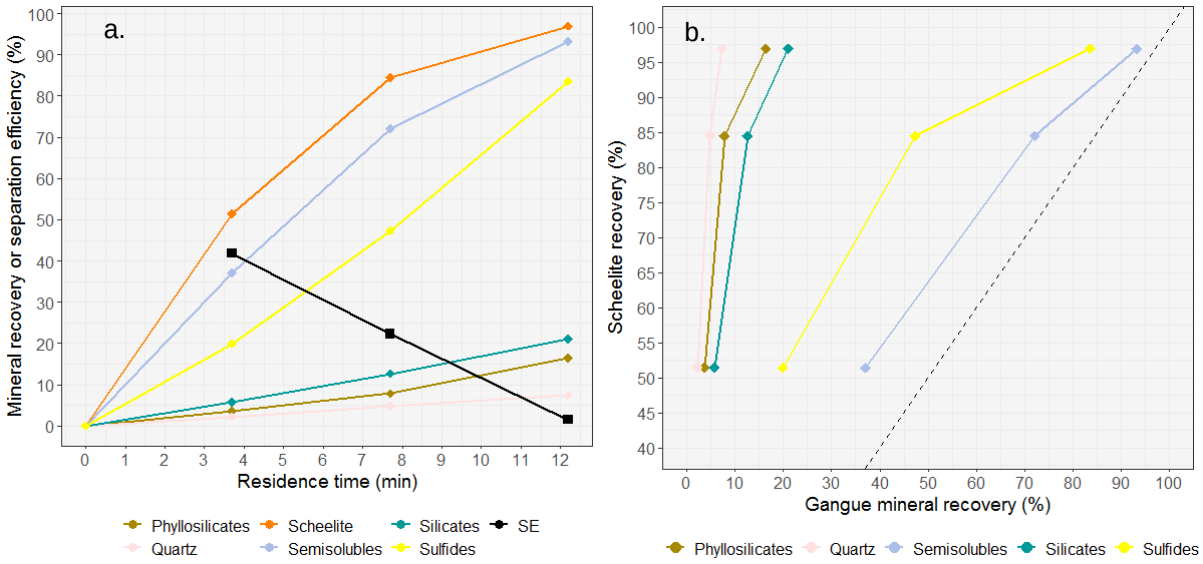

Figure 7: a) Cumulative mineral recoveries and separation efficiency (SE, non-cumulative) and b) selectivity curves, the three points represent the three concentrate streams and the dotted line is the selectivity line

The flotation rate constant k was calculated for all minerals based on the classical first order kinetics equation (Sutherland, 1948) (Table 2). It confirms the previous observations. All salt-type-type minerals show the highest flotation rate constants while the silicates (specifically quartz) show little floatability. Using R, any model can be applied to any number of particle size classes.

Table 2: Calculated flotation rate constant k and associated maximum recovery at infinite flotation time R_{max}

	R_{max} (%)	**k (min^{-1})**
Phyllosilicates	31.7	0.0483
Quartz	16.9	0.0449
Scheelite	100	0.22
Semi-solubles	100	0.16
Silicates	37.7	0.0588
Sulfides	100	0.099

Beyond the potential issue of the depressant, the fact that the ore is ground so fine may also have an impact. Mineral recoveries and separation efficiency per size class are plotted in Figure 8. A clear difference between minerals floating through true flotation or mechanically through entrainment is observed. Scheelite is very well recovered independently of the size class, with a small peak between 40 and 80 µm, which could be considered as the minimum particle size required for flotation. Semi-soluble salt-type minerals also float uniformly except in the largest particle size class, where mineral association might interfere. Sulfides are recovered in the finer size classes, just like the other gangue minerals but at a much higher rate. The separation efficiency increases with particle size, which is expected as finer particles are known to be more affected by entrainment.

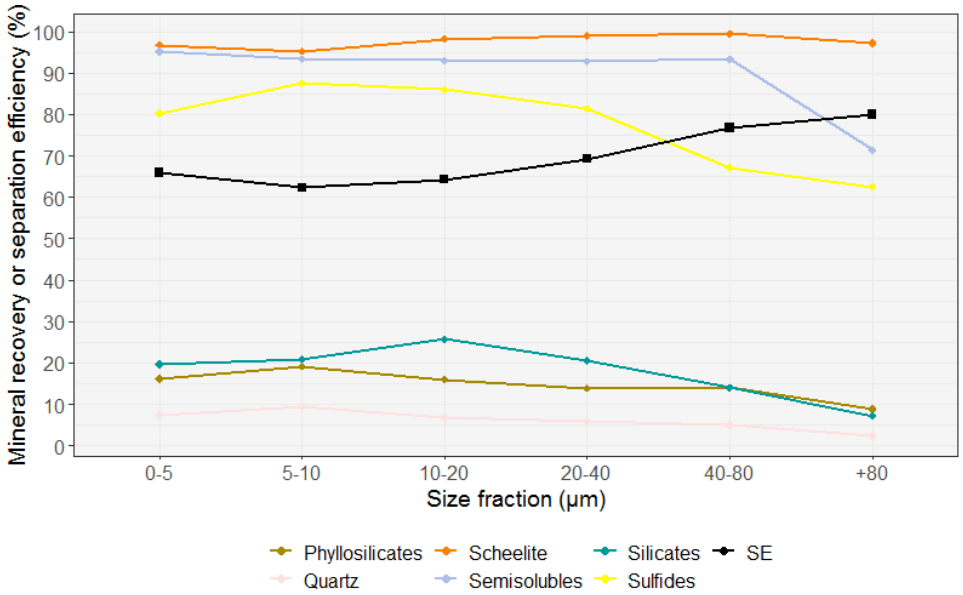

Figure 8: Mineral recoveries and separation efficiency (SE) based on the size fractions in the rougher concentrate

Selected mineral recoveries per size class over time are plotted in Figure 9. Scheelite displays very different behavior over time and most of it is recovered within the two first sets of cells with a clear peak at 40 to 80 µm shifting to +80 µm. The contrast is not as obvious in the last four cells, where roughly 20% of the remaining scheelite floats. Gangue minerals tend to display a peak fraction at which they are “best” recovered, 10 to 20 µm for the silicates or 5 to 10 µm for phyllosilicates and quartz. Residence time has very little impact on the flotation of gangue minerals as they float relatively uniformly over the sets of cells. These observations indicate that there is potentially some overgrinding in the process. Reduced grinding would possibly lead to a more selective flotation even if the surface liberation is affected, as it was shown that 40% free surface were largely enough for scheelite to float.

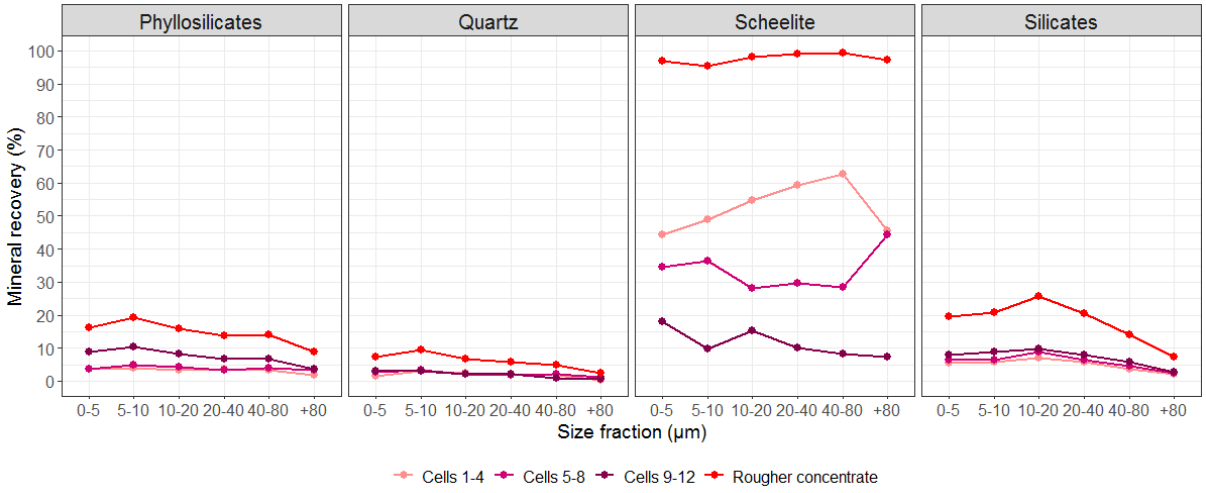

Figure 9: Recoveries of scheelite and different gangue mineral groups based on particle size

4.2. *Entrainment*

To further understand the behaviour of the hydrophilic minerals, it is possible to calculate an entrainment factor (ent) for the main gangue minerals of the ore (Table 3). Entrainment decreases over time for albite, augite and quartz but increases for all other gangue minerals. Serpentine has the highest entrainment of all. Anorthite, titanite and augite are silicates with high calcium content: their high to moderate entrainment may indicate a more complex behaviour than simple mechanical entrainment.

Entrainment is in general highly correlated with pulp density but independent of water recovery Rw as shown by Wang (2016). Quartz is possibly more affected by liquid velocity at the pulp-froth interface than the rest of the gangue minerals, as it is the only mineral whose recovery is correlated with the water recovery. The reason for this is unclear.

Table 3: Entrainment for the main gangue minerals with the associated cell parameters (Rw = water recovery, ent = entrainment)

Stream	Cell parameters		Entrainment							
	Pulp density (%)	Rw (%)	Albite	Anorthite	Augite	Biotite	Hornblende	Quartz	Serpentine	Titanite
Cells 1-4	47.55	9.43	0.40	0.82	0.65	0.29	0.45	0.19	1.22	1.03
Cells 5-8	46.07	10.68	0.37	0.99	0.66	0.29	0.45	0.19	1.38	1.06
Cells 9-12	42.18	12.27	0.38	1.70	0.55	0.48	0.63	0.17	2.79	1.81
Total concentrate	45.12	32.38	0.37	1.06	0.55	0.33	0.51	0.22	1.73	1.22
Mineral density			2.60	2.75	3.2 - 3.6	2.8 - 3.4	2.9 - 3.4	2.65	2.5 - 3.3	3.5 - 3.6
Correlation water/ent			-0.53	-0.04	-0.66	-0.04	0.11	0.82	0.05	-0.01
Correlation pulp density/ent			0.56	-0.98	0.77	-0.94	-0.96	0.45	-0.98	-0.96

Figure 10 shows that the coarsest particles are less entrained even if particles entrained are coarser over time. Zheng et al. (2006) claimed that "*within the normal range of cell operating conditions, few particles coarser than 50 µm are recovered by entrainment*". Though this is compatible with our results, such statements should naturally be taken with caution (Wiese and O'Connor, 2016). Entrainment of titanite, anorthite and serpentine increases over time, which is mainly linked to the 5 to 10 and 10 to 40 µm size classes. It also increases slightly for hornblende and biotite but remains similar for quartz and albite.

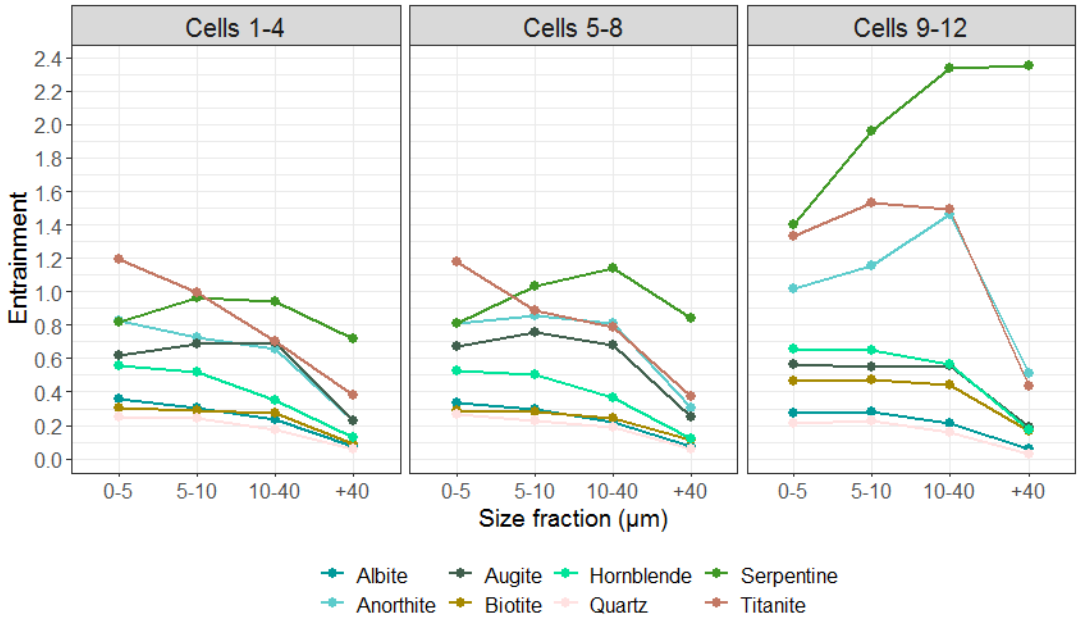

Figure 10: Entrainment factor per size fraction for the main gangue minerals over time (lines are to guide the eye)

Entrainment is also linked to particle shape, e.g. Wiese et al. (2015) and Kirjavainen (1992). Based on the method established by Little et al. (2016), a modified entrainment factor based on shape classes was calculated, not just for roundness but also for the other shape factors (Figure 11). Each shape class has an average number of particles of 2,200.

Figure 11 shows clearly that entrainment increases with particle roundness, similarly to Little et al. (2016) but in contrast to Wiese et al. (2015) and Vizcarra et al. (2011), especially for quartz and for titanite. Based on the results of this study, it seems obvious that anorthite and titanite (calcium silicates) are partially floated through true flotation, even if the main mechanism of their flotation remains entrainment. On the other hand, the high entrainment of serpentine seems independent of its shape as its Ent_j curve is flatter than other minerals'.

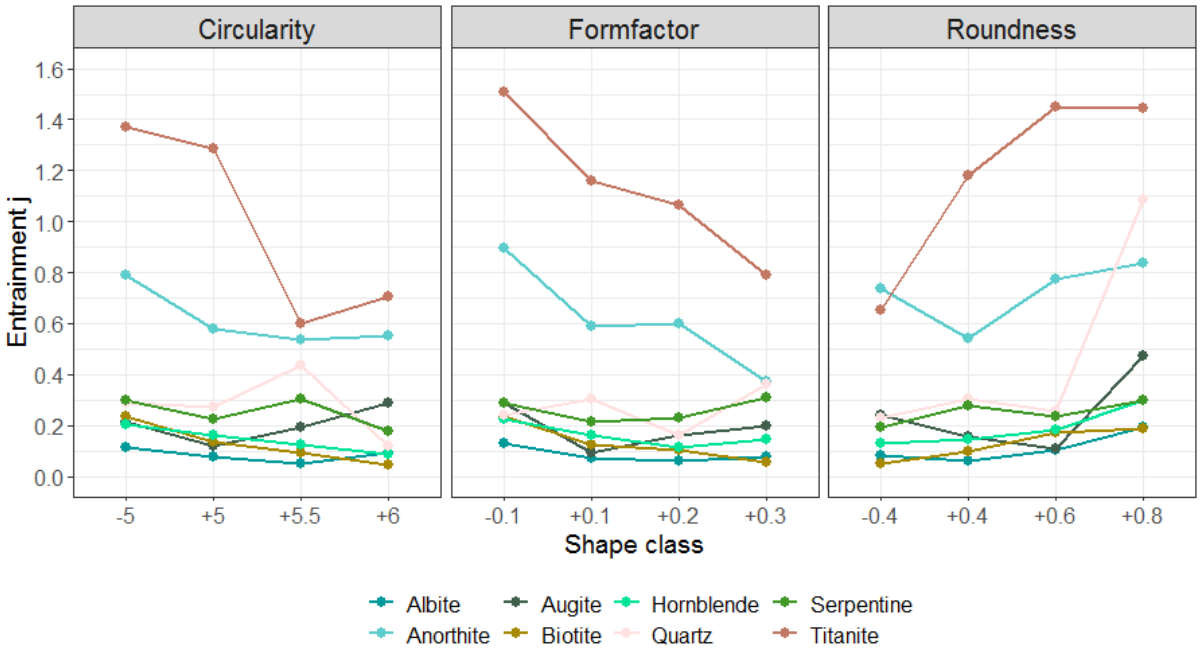

Figure 11: Modified entrainment factor based on shape class for circularity and roundness (lines to guide the eye)

Based on Figure 6 and Figure 11, high roundness and to a lesser extent, low circularity and lower form factor increase the likelihood that hydrophilic minerals are floated via entrainment. The mechanism here is unclear: it could be linked to the behavior of a round particle in regards to the hydrodynamics of the pulp (a rounder particle will offer less resistance to the flows and be more easily carried to the froth) or to froth fractionation (the shape of the particle and the froth height will affect how particles are drained back to the pulp as shown in Redlinger-Pohn et al. (2016)).

5. Conclusions

The performance of an industrial rougher flotation bank was described using R-assisted statistical analysis of automated mineralogy data, with tungsten-bearing scheelite as the target mineral. This approach provides more in-depth information than the traditional approaches and at higher calculation speed than with a classic spreadsheet. The R routines used are also powerful tools for flexible diagram generation achieved at any level of aggregation required.

As a summary, based on the observations and under the current reagent regime, ideally floating scheelite particles are coarser than 40 µm and have a surface liberation degree above 40%. Most of the scheelite lost to the rougher tailings stream is either ultrafine or coarse with little surface liberation and associated with silicates. More importantly, even with the presence of a depressant, the selectivity over other calcium-bearing semi-soluble salt-type minerals is close to zero. This is linked to particle size, as there appears to be some overgrinding before the rougher flotation. While the impact of the depressant requires more observation, less fine grinding could potentially improve the concentrate grade and decrease operational costs.

This article shows how particle statistical analysis can be used to go beyond the restrictions of discrete property classes. In the future, the authors are looking at using non-parametric statistical methods to flexibly predict the recovery of specific minerals as a function of their grain or particle size, their surface liberation and their shape. These techniques will also be applied under different hydrodynamic and chemical conditions to analyze the impact of these changing conditions on flotation. Finally, the statistical reliability of the results remains an open issue: bootstrap resampling may be used to assess said statistical reliability as demonstrated in Buchmann et al. (2018).

6. Acknowledgements

This paper was partially written thanks to the financial support of the OptimOre project. Said project has received funding from the European Union's Horizon 2020 research and innovation program under grant agreement no°642201. The authors would like to thank their research assistants Adrian and Ana Paula for taking care of the sample preparation and the beneficiation plant for allowing the use of their data for research purposes.

7. Literature

Buchmann, M., Schach, E., Tolosana-Delgado, R., Leißner, T., Astoveza, J., Kern, M., Möckel, R., Ebert, D., Rudolph, M., Van den Boogaart, K.G., Peuker, U.A., Evaluation of Magnetic Separation Efficiency on a Cassiterite-Bearing Skarn Ore by Means of Integrative SEM-Based Image and XRF–XRD Data Analysis. Minerals, 2018, **8(9)**, 390.

Butcher, A., 2015. A short history of automated mineralogy colours, Blogspot.

Fandrich, R., Gu, Y., Burrows, D., Moeller, K., Modern SEM-based mineral liberation analysis. International Journal of Mineral Processing, 2007, **84(1–4)**, 310-320.

FEI, 2014. MLA Image Processing, 3.1.4.686 ed. FEI Company, Hillsboro, United States.

Greet, C.J., 2013. Virtual sizing: the wrong way to complete liberation analysis, In *Flotation13*, ed. Wills, B.A. MEI, Cape Town, South Africa.

Heinig, T., Bachmann, K., Tolosana-Delgado, R., Van den Boogaart, K.G., Gutzmer, J., 2015. Monitoring gravitational and particle shape settling effects on MLA sample preparation, In *IAMG Conference 2015*, Freiberg, Germany.

Kirjavainen, V.M., Mathematical model for the entrainment of hydrophilic particles in froth flotation. International Journal of Mineral Processing, 1992, **35(1)**, 1-11.

Kopf, D., 2017. If you want to upgrade your data analysis skills, which programming language should you learn? Quartz.

Kupka, N., Rudolph, M., Froth flotation of scheelite - A review. International Journal of Mining Science and Technology, 2018, **28(3)**, 373-384.

Little, L., Wiese, J., Becker, M., Mainza, A., Ross, V., Investigating the effects of particle shape on chromite entrainment at a platinum concentrator. Minerals Engineering, 2016, **96-97**, 46-52.

Lotter, N.O., Modern Process Mineralogy: An integrated multi-disciplined approach to flowsheeting. Minerals Engineering, 2011, **24(12)**, 1229-1237.

Pereira, L., Birtel, S., Möckel, R., Michaux, B., Silva, A.C., Gutzmer, J., Constraining the Economic Potential of By-Product Recovery by Using a Geometallurgical Approach: The Example of Rare Earth Element Recovery at Catalão I, Brazil. Economic Geology, 2019.

Pourghahramani, P., Forssberg, E., Review of applied particle shape descriptors and produced particle shapes in grinding environments. Part I: Particle shape descriptors. Mineral Processing and Extractive Metallurgy Review, 2005, **26(2)**, 145-166.

Quinteros, J., Wightman, E., Johnson, N.W., Bradshaw, D., Evaluation of the response of valuable and gangue minerals on a recovery, size and liberation basis for a low-grade silver ore. Minerals Engineering, 2015, **74**, 150-155.

Rao, K.H., Forssberg, K.S.E., 1992. Interactions of Anionic Collectors in Flotation of Semi-Soluble Salt Minerals, In *Innovations in Flotation Technology*, eds. Mavros, P., Matis, K.A. Springer Netherlands, Dordrecht, pp. 331-356.

RCoreTeam, 2016. R: A language and environment for statistical computing. R Foundation for Statistical Computing, Vienna, Austria.

Redlinger-Pohn, J.D., Grabner, M., Zauner, P., Radl, S., Separation of cellulose fibres from pulp suspension by froth flotation fractionation. Separation and Purification Technology, 2016, **169**, 304-313.

Rolando, L., William, P., Mineralogical Characterization of Sieved and Un-Sieved Samples. Journal of Mienrals and Materials Characterization and Engineering, 2014, **2(1)**, 40-48.

Schach, E., Buchmann, M., Tolosana-Delgado, R., Leißner, T., Kern, M., Gerald van den Boogaart, K., Rudolph, M., Peuker, U.A., Multidimensional characterization of separation processes – Part 1: Introducing kernel methods and entropy in the context of mineral processing using SEM-based image analysis. Minerals Engineering, 2019, **137**, 78-86.

Sutherland, K.L., Physical chemistry of flotation. XI: Kinetics of the flotation process. Journal of Physical and Colloid Chemistry, 1948, **52(2)**, 394-425.

Vizcarra, T.G., Harmer, S.L., Wightman, E.M., Johnson, N.W., Manlapig, E.V., The influence of particle shape properties and associated surface chemistry on the flotation kinetics of chalcopyrite. Minerals Engineering, 2011, **24(8)**, 807-816.

Vos, C., Evans, C., Wightman, E., Knappes, R., Manlapig, E.V., Bradshaw, D., 2015. Characterizing mineral particle perimeter texture for flotation, In *Flotation Conference*. MEI, Cape Town.
Wang, L., 2016. Entrainment of Fine Particles in Froth Flotation, In *Sustainable Minerals Institute*. University of Queensland, Australia, p. 181.
Wiese, J., Becker, M., Yorath, G., O'Connor, C., An investigation into the relationship between particle shape and entrainment. Minerals Engineering, 2015, **83**, 211-216.
Wiese, J., O'Connor, C., An investigation into the relative role of particle size, particle shape and froth behaviour on the entrainment of chromite. International Journal of Mineral Processing, 2016, **156**, 127-133.
Wills, B.A., Finch, J., *Wills' Mineral Processing Technology - An Introduction to the Practical Aspects of Ore Treatment and Mineral Recovery*. Eighth Edition edn. 2016, Butterworth-Heinemann.
Yianatos, J., Contreras, F., Particle entrainment model for industrial flotation cells. Powder Technology, 2010, **197(3)**, 260-267.
Zheng, X., Franzidis, J.P., Johnson, N.W., Modelling of entrainment in industrial flotation cells: Water recovery and degree of entrainment. Minerals Engineering, 2006, **19(11)**, 1191-1203.

Annex 1: Mineralogical composition per size fraction quantiles of each stream

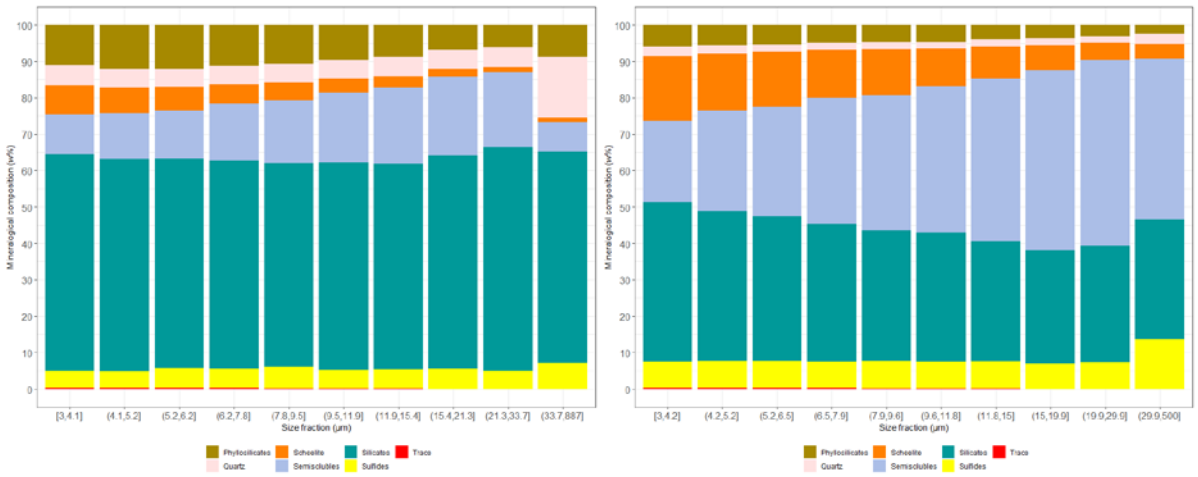

Figure 12: a) Rougher feed, b) Cells 1-4

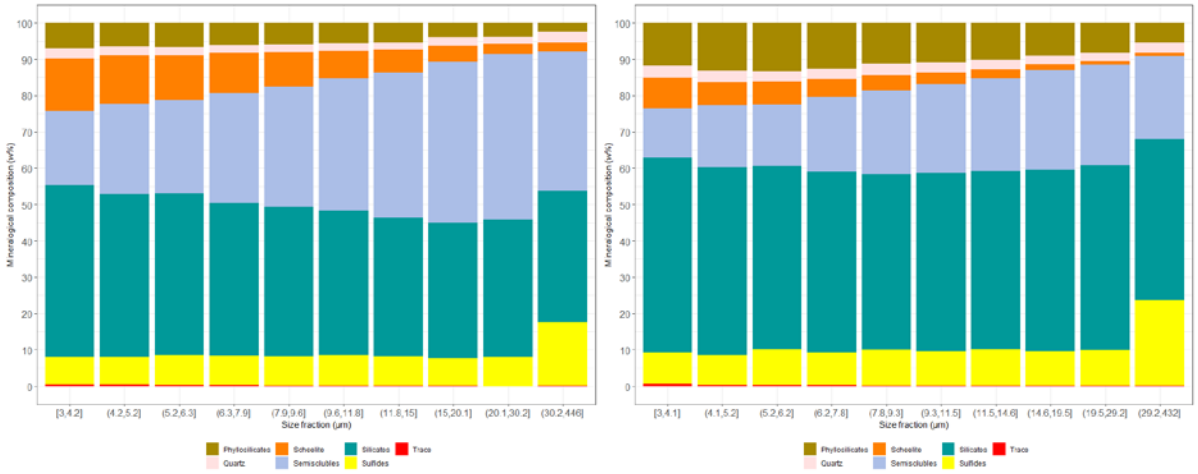

Figure 13: a) Cells 5-8, b) Cells 9-12

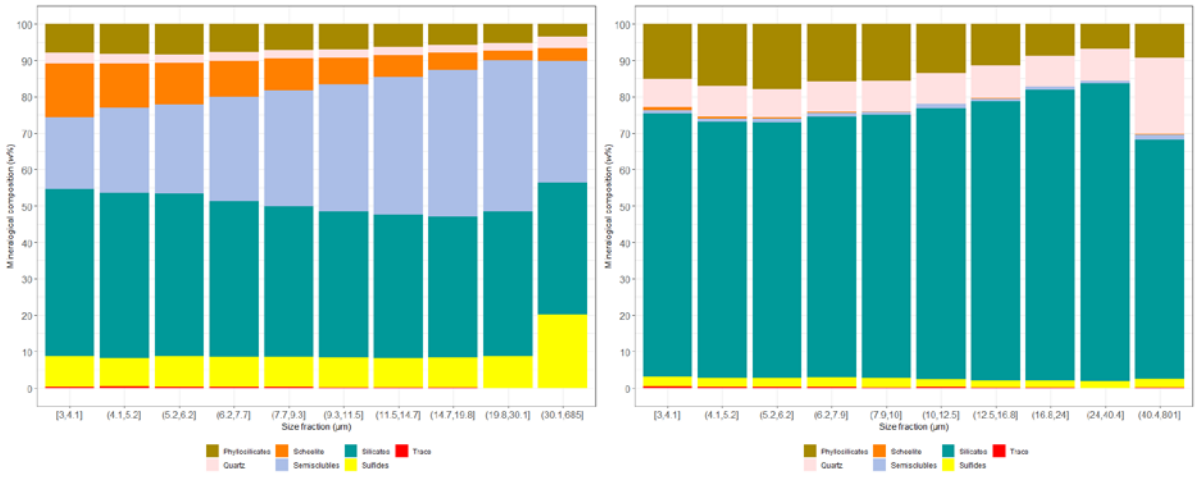

Figure 14: a) Rougher concentrate, b) Rougher tailings